Brain Stimulation 15 (2022) 1269–1278

Contents lists available at ScienceDirect

Brain Stimulation

journal homepage: http://www.journals.elsevier.com/brain-stimulation

Restoration of functional network state towards more physiological condition as the correlate of clinical effects of pallidal deep brain stimulation in dystonia

Pavel Filip [a, b, *, 1], Robert Jech [a, **, 1], Anna Fečíková [a], Petra Havránková [a], Filip Růžička [a], Karsten Mueller [a, c], Dušan Urgošík [a, d]

[a] Department of Neurology, Charles University, First Faculty of Medicine and General University Hospital, Prague, Czech Republic
[b] Center for Magnetic Resonance Research (CMRR), University of Minnesota, Minneapolis, MN, USA
[c] Max Planck Institute for Human Cognitive and Brain Sciences, Leipzig, Germany
[d] Department of Stereotactic and Radiation Neurosurgery, Nemocnice Na Homolce, Prague, Czech Republic

ARTICLE INFO

Article history:
Received 22 March 2022
Received in revised form
7 August 2022
Accepted 31 August 2022
Available online 9 September 2022

Keywords:
Deep brain stimulation
Dystonia
Internal globus pallidus
Resting-state functional magnetic resonance imaging
Connectivity

ABSTRACT

Background: Deep brain stimulation of the internal globus pallidus (GPi DBS) is an invasive therapeutic modality intended to retune abnormal central nervous system patterns and relieve the patient of dystonic or other motor symptoms.
Objectives: The aim of the presented research was to determine the neuroanatomical signature of GPi DBS modulation and its association with the clinical outcome.
Methods: This open-label fixed-order study with cross-sectional validation against healthy controls analysed the resting-state functional MRI activity changes induced by GPi DBS in 18 dystonia patients of heterogeneous aetiology, focusing on both global (full brain) and local connectivity (local signal homogeneity).
Results: Compared to the switched-off state, the activation of GPi DBS led to the restoration of global subcortical connectivity patterns (in both putamina, diencephalon and brainstem) towards those of healthy controls, with positive direct correlation over large-scale cortico-basal ganglia-thalamo-cortical and cerebellar networks with the clinical improvement. Nonetheless, on average, GPi DBS also seemed to bring local connectivity both in the cortical and subcortical regions farther away from the state detected in healthy controls. Interestingly, its correlation with clinical outcome showed that in better DBS responders, local connectivity defied this effect and approached healthy controls.
Conclusions: All in all, the extent of restoration of both these main metrics of interest towards the levels found in healthy controls clearly correlated with the clinical improvement, indicating that the restoration of network state towards more physiological condition may be a precondition for successful GPi DBS outcome in dystonia.
© 2022 The Author(s). Published by Elsevier Inc. This is an open access article under the CC BY license (http://creativecommons.org/licenses/by/4.0/).

Abbreviations: MRI, magnetic resonance imaging; T1w, T1-weighted; rs-fMRI, resting-state functional magnetic resonance imaging; DBS, deep brain stimulation; GPi, internal globus pallidus; HC, healthy controls; DY, dystonia patients; GloCon, global connectivity; LocCon, local connectivity; VTA, Volume of Tissue Activated; VTA-Con, seed-based functional connectivity of the VTA region; ROI, Region of Interest; BFMDS, Burke-Fahn-Marsden Dystonia Scale; TWSTRS, Toronto Western Spasmodic Torticollis Rating Scale; MNI, Montreal Neurological Institute; CIFTI, Connectivity Informatics Technology Initiative; HCP, Human Connectome Project; tSNR, temporal Signal-to-Noise Ratio; FBER, Foreground-Background Energy Ratio; FDR, False Discovery Rate.

* Corresponding author. Department of Neurology, First Faculty of Medicine Charles University and General University Hospital in Prague Kateřinská 30, 120 00, Prague, Czech Republic.
** Corresponding author. Department of Neurology, First Faculty of Medicine Charles University and General University Hospital in Prague Kateřinská 30, 120 00, Prague, Czech Republic.
E-mail addresses: pvlfilip@gmail.com (P. Filip), jech@cesnet.cz (R. Jech).
[1] Authors contributed equally to the study.

https://doi.org/10.1016/j.brs.2022.08.025
1935-861X/© 2022 The Author(s). Published by Elsevier Inc. This is an open access article under the CC BY license (http://creativecommons.org/licenses/by/4.0/).

1. Introduction

Dystonia is clinically defined as a movement disorder with sustained or intermittent muscle contractions leading to abnormal, often repetitive movements, postures or both [1]. The currently leading hypothesis on its neurophysiological basis, though still debated, is that of a network disorder encompassing cortico-basal ganglia-thalamo-cortical and cerebellar networks [2]. Despite the absence of marked, readily visible structural alterations in conventional clinical MRI scans, which may even be considered a clinical hallmark of dystonia, data from more precise neuroimaging and anatomical studies support the previous notion, reporting differences in the volume of basal ganglia, cerebellum and cortical structures in patients with isolated dystonias [3–5]. Furthermore, functional MRI studies have also repeatedly pointed to these key regions responsible for sensorimotor processing and integration [6].

Similarly, the view on the mechanisms of action of DBS in general has recently undergone a paradigm shift from localised stimulation and/or inhibition effects towards global modulation of large-scale brain networks [7]. However in dystonia, despite its generally good, sustained clinical effects, with improvement of both motor and functional scales [8], the exact nature of network alterations induced by GPi DBS remains unclear. Unlike in essential tremor or Parkinson's disease, where DBS response is often very rapid, a reasonable clinical benefit in dystonia may appear only after several weeks of stimulation, especially in tonic dystonic components. Intracortical $GABA_A$-mediated inhibition takes up to six months to improve to normal levels, in correlation with the clinical benefit development in GPi DBS dystonia patients [9], similarly to the normalisation of long-term potentiation in the motor cortex [10], both pointing to more extensive changes and complex neuroplasticity-associated processes elicited by GPi DBS [11].

Hence, the presented study was designed to further evaluate network effects of GPi DBS in dystonia (DY) patients. To this aim, patients with DY of various aetiology, previously indicated for GPi DBS within the standard clinical workflow, were retrospectively enrolled to undergo resting-state functional MRI (rs-fMRI) acquisition with active GPi DBS followed by a rs-fMRI session with DBS switched off. The following aims were set:

1) Evaluation of the relationship between the position of the DBS electrodes in the target GPi region and the clinical effect of DBS.
2) Delineation of the effect of GPi DBS on:
   a. Global Connectivity (GloCon), a centrality measure defining the number of connections in the whole network, with the intent to evaluate the alterations at the level of the whole brain; and
   b. Local Connectivity (LocCon) as a measure of spatially delimited, local correlation of rs-fMRI signal fluctuations, a proxy of local neuronal population synchronisation, which was chosen to provide information on more localised alterations.
3) Assessment whether DBS-induced changes of rs-fMRI metrics corresponded to the restoration of healthy network state, i.e. DBS brought the network state closer to the condition seen in healthy controls (HC), who were separately acquired for the purposes of this study, or elicited a qualitatively different pattern.
4) Correlation of DBS-induced alterations of rs-fMRI metrics with the clinical improvement evaluated using established clinical scales.

Our primary hypothesis postulated that GPi DBS would lead to restoration of physiological network state, and its extent would be directly proportional to the clinical improvement.

2. Methods

2.1. Subjects

23 DY patients (seven females, median age [range] of 43.5 [16–76]) under chronic DBS therapy and 23 age and sex-paired HC (seven females, 41.5 [21–75]) were enrolled into this study. DY patients had been diagnosed by a tertiary-care movement disorders centre specialist according to the latest diagnostic criteria [1]. DY-specific inclusion criteria were the presence and/or history of dystonia regardless of its aetiology, bilateral GPi DBS implantation indicated for dystonia management and its activation at least six months before the participation in this study, stable DBS programming parameters for at least one month before the participation in this study and no head tremor (to avoid imaging artifacts). Common exclusion criteria relevant for both DY and HC subjects were the following: general contraindications to MRI examination (other than the presence of a full implanted DBS system), the presence of a non-negligible vascular or space occupying lesion in brain MRI scans and a neurological and/or psychiatric disorder other than the diagnosis related to dystonic symptoms. The main clinical data of interest were one of the following two scales: Burke-Fahn-Marsden Dystonia Scale [BFMDS] [12] or Toronto Western Spasmodic Torticollis Rating Scale [TWSTRS] [13] chosen based on the clinical presentation of each DY subject. The evaluation of the clinical condition was performed at three separate occasions – before DBS implantation, before DBS-ON MRI acquisition and before DBS-OFF MRI acquisition). The clinical effect of DBS was expressed as percentual clinical score change calculated as the ratio of the difference of the relevant clinical score before DBS implantation and immediately before the DBS-ON MRI session to the score before DBS implantation.

Every subject signed a written informed consent form as customary according to the Declaration of Helsinki. The study protocol was approved by the ethics committee of the General University Hospital in Prague.

2.2. Imaging protocol and data analysis

For the full imaging and data processing protocol, see the supplementary material.

Briefly, a 1.5 T S Symphony System (Siemens, Erlangen, Germany) was utilised to acquire a T1-weighted (T1w) structural scan and a rs-fMRI session, with gradient-recalled echo echo-planar imaging sequence, in-plane resolution 3×3 mm^2, slice thickness 3 mm, 1 mm interslice gap, 31 slices, TR 3000 ms, TE 51 ms, FA 90°, 200 volumes. DY patients were scanned in two separate sessions separated by approximately 2 h: rs-fMRI acquisition with active DBS utilising the stimulation parameters as recommended by the attending physician (DBS-ON session) and rs-fMRI acquisition with DBS switched off (DBS-OFF session).

Lead-DBS software [14] with the enhanced workflow [15] was used to determine the position of DBS leads and active contacts. The correlation of the position of the active contact and the clinical effect of DBS was based on the parameter “Impact of DBS” [16]. Volume of Tissue activated (VTA) binary mask was extracted for each subject to be used in the following connectivity analysis (see below).

rs-fMRI pre-processing included slice timing correction, the realignment of the timeseries to correct for subject motion and co-registration to the structural T1w scan combined with T1w-derived

warp into the Montreal Neurological Institute (MNI) space. In the following steps, the volume timeseries were mapped to the standard CIFTI grayordinate space, as described in the fMRISurface step of Human Connectome Project (HCP) Minimal Preprocessing Pipeline [17]. The subsequent processing was based on the HCP rs-fMRI pipeline [18], consisting of MELODIC independent component analysis and automatic artefactual components identification via the FIX algorithm [19].

Out of the 23 enrolled DY subjects, two DY subjects failed to complete the full MRI protocol, 2 DY subjects had insufficient brain coverage with good fMRI signal (<80%, see Supplementary Fig. 1). One subject had suboptimal position of one DBS lead missing the target region with all the contacts, requiring subsequent reimplantation of the lead. These five subjects and their age and sex-paired HC were excluded from the final analysis, leaving 18 DY subjects and 18 HC for the following processing.

The AFNI package [20] was used to calculate voxel/vertex-wise weighted degree centrality as a measure of GloCon with sparsity threshold of 0.1 [21]. A combined parameter labelled LocCon was calculated as Kendall's W over 27 neighboring voxels [22] for voxel-coded subcortical structures in the CIFTI files and as vertex-wise concordance within a prespecified range of geodesic distance up to 20 mm for the cortical structures. The third, exploratory parameter of interest, seed-based connectivity map of DBS VTA (VTA-Con) was calculated only for DY subjects as Fisher transformation of voxel/vertex-wise Pearson's coefficient of correlation with the mean signal time course over combined DBS VTA region of interest (ROI) (left and right-side).

In the last step, the processed outputs (GloCon, LocCon, VTA-Con) were parcellated using a combination of HCP-derived cortical parcellation consisting of 180 parcels per hemisphere [23] and resting-state network-based sub-segmentation of Freesurfer-derived subcortical grey matter structures (in total 68 subcortical sub-segments).

2.3. Statistical analysis

Descriptive statistics was used to summarise quantitative demographic and clinical data for all eligible subjects (see Table 1).

The Aim 1 was evaluated using Pearson's coefficient of correlation of normalised Impact of DBS in preselected ROIs (whole GPi, sensory part of GPi and motor part of GPi) with the percentual clinical score change. The analysis of the Aims 2 and 4 was based on one repeated-measures general linear model (GLM) for the three main rs-fMRI parameters (GloCon, LocCon, VTA-Con) with two session groups (DY DBS-ON, DY-DBS-OFF) and percentual clinical score change as fixed factors. Furthermore, the following parameters of non-interest were included in this GLM: sex, age, body distribution (cervical/generalised) and disease duration. And lastly, the Aim 3 was evaluated using two further GLMs for GloCon and LocCon, containing subject group (HC vs DY DBS-ON and HC vs DBS-OFF in two separate GLMs) and the following covariates of non-interest: age, sex and subject-specific temporal signal-to-noise ratio (tSNR) over the whole brain calculated from fully pre-processed data to account for the significant difference in this factor between the HC and both DY DBS-ON and DY DBS-OFF sessions.

For the Aim 1, false discovery rate (FDR) correction [24] over the 3 considered ROIs was utilised. For the Aims 2, 3, and 4 a combined FDR correction over voxels/vertices, contrasts and modalities was implemented [25]. For the Aim 1, 2 and 4, the results were considered significant at the level of $p < 0.05$ and for the Aim 3, a type I error threshold of 0.01 was implemented due to non-negligible difference in MRI data quality between HC and DY subjects.

3. Results

Basic demographic and clinical information is presented in Table 1. Even though discouraged in the current dystonia classification guidelines [1], the figures presented in this paper generally distinguish between “primary” dystonia (this group included idiopathic cervical and generalised dystonia and DYT-TOR1A patients, in total 14 subjects) and “secondary” dystonia (parkinsonism plus, PKAN and postanoxic dystonia, in total four subjects) for better overview.

3.1. Aim 1 – DBS electrode placement and its clinical correlation

In all eligible DY subjects, DBS electrodes were placed in the GPi region as defined by the DISTAL atlas [26] (see Fig. 1A and 1.B for the representation of active contact centres over 3D GPi reconstruction). The overlap of VTA and GPi was 41.1% of VTA [25.1–100%] (median [10th-90th percentile]) and the Impact of DBS reached 2,110,827 [261,585–4,649,461]. The correlation analysis of the Impact of DBS and the percentual clinical score change revealed mild positive, but statistically non-significant correlation for the whole GPi ($r = 0.310$; $p(FDR) = 0.316$) and motor part of GPi ($r = 0.208$; $p(FDR) = 0.408$), and significant positive correlation for the sensory part of GPi ($r = 0.618$; $p(FDR) = 0.019$) (see Fig. 1C). As seen in Fig. 1C, the exclusion of the secondary dystonia from the correlation analysis did not lead to substantial changes of the correlation trendline slope (full vs dashed line).

3.2. Aim 2 - difference in rs-fMRI metrics between DBS-ON and DBS-OFF condition

As depicted in Fig. 2A, DY subjects had significantly higher GloCon in both putamina, thalami, ventral diencephalon and the cerebellum. Furthermore, there were two cortical areas with increased connectivity: in the left middle cingulate and left frontal pole (see also Table 2 and Supplementary Table 3 for the full list of significant areas, anatomical localisation and statistical significance, including relevant ranges of respective metrics). LocCon exhibited more complex alterations, with decreased signal homogeneity in large cortical areas in bilateral frontal, parietal and temporal lobes during the DBS-ON session, but increased signal homogeneity in both putamina, ventral diencephalon, brainstem and left thalamus. And lastly, VTA-Con was higher in DBS-ON in both putamina and thalami, in the right premortor cortex and both occipital lobes. Furthermore, there were small areas of lower VTA-Con in frontal pole, brainstem and ventral diencephalon.

3.3. Aim 3 – difference in rs-fMRI metrics between HC and DY

As shown in Fig. 2C and Fig. 3B.I, the increase of GloCon detected in the DY DBS-ON > DBS-OFF contrast constituted a partial restoration of the metric in putamen, ventral diencephalon and cerebellum towards the state seen in HC (see also the Supplementary Table 4). Cortical differences between HC and DY in bilateral frontal, parietal and temporal lobes and cingulate were detectable in similar extent in both HC > DY DBS-OFF and HC > DBS-ON contrasts. On the other hand, the increase of LocCon in bilateral putamina detected in the DY DBS-ON > DBS-OFF contrast was in the direction opposite the HC level (see Fig. 3B.II). Similarly, cortical LocCon differences in the contrast HC > DBS-ON were present in more areas than in the contrast HC > DBS-OFF (see Fig. 2), again pointing to DBS-induced deviation from the norm.

Table 1
Basic demographic and clinical data. Only eligible subjects (not excluded in previous quality control steps) are considered in this table. Continuous data displayed as median [range], categorical variables as numbers of subjects in the relevant group. Abbreviations: M – male; F – female; V – Volt, mA – milliampere; us – microsecond; Hz – Hertz; Ω - Ohm; DBS – deep brain stimulation; TWSTRS – Toronto Western Spasmodic Torticollis Rating Scale; BFMDS – Burke-Fahn-Marsden Dystonia Scale; N/A – TWSTRS data not available/relevant for secondary dystonia patients, since all the subjects in this group had generalised symptoms.

	Dystonia patients	Healthy controls
Sex **(M/F)**	11/7	11/7
Age	43.5 [16–76]	41.5 [21–75]
Axis I		
Age of onset (years)	27 [8–66]	
Disease duration (years)	12 [1–27]	
Body distribution [cervical/generalised]	7/11	
Associated features [none/parkinsonism/other]	14/3/2	
Axis II		
Neurodegeneration/Static CNS lesions/None	3/1/14	
Inherited/Acquired/Idiopathic sporadic	2/1/15	
Medication		
Anticholinergics/Baclofen/Antiepileptic drugs	5/2/2	
Benzodiazepines/Antidepressants	10/11	
L-dopa/Dopamine agonist	1/1	
DBS-related information		
Stimulator type [Libra/Brio/Kinetra/RC Activa]	1/3/4/10	
Lead type [Abbott/St Jude active tip 6142–6149/Medtronic 3389]	4/14	
Time since implantation (months)	34 [9–95]	
DBS response as evaluated by the attending physician **[non-responder/partial responder/responder]**	8/3/7	
Stimulation mode [monopolar/bipolar/interleaved]	16/1/1	
Constant voltage/constant current mode	9/9	
Voltage amplitude (V) – bilateral average	1.8 [1.2–3.1]	
Current (mA) – bilateral average	1.5 [1.1–2.3]	
Pulse width (us)	212 [162–450]	
Frequency (Hz)	130 [50–130]	
Impedance (Ω) – only available in 13 subjects	878 [400–1726]	
	Primary dystonia	**Secondary dystonia**
TWSTRS (in relevant subjects)		
Before DBS implantation	24 [24–29]	N/A
DBS-ON	14 [0–21]	N/A
DBS-OFF (2 h after switching off)	21 [14–26]	N/A
BFMDS (in relevant subjects)		
Before DBS implantation	29 [8–50]	28 [4–71]
DBS-ON	17 [0–37]	27 [4–84]
DBS-OFF (2 h after switching off)	19 [0–37]	27 [4–88]
Percentual clinical scale improvement with DBS		
Before DBS implantation vs DBS-ON (%)	47.7 [-25.9–100.0]	−11.8 [-19.1–9.0]
DBS-OFF vs DBS-ON (%)	21.0 [0.0–100.0]	0.0 [0.0–4.5]

3.4. Aim 4 – interaction of the effect of DBS-ON vs OFF in rs-fMRI metrics with clinical score change

Clinical improvement positively correlated with the increase of connectivity (GloCon) over virtually all the major cortical areas, in the bilateral putamen, ventral diencephalon, cerebellum and brainstem (see Fig. 2B, Table 2 and Supplementary Table 3). This correlation was also present when distinguishing between the primary and secondary DY group (see Fig. 3A.I and 3.A.III). However, LocCon exhibited an inverse correlation between DBS-induced

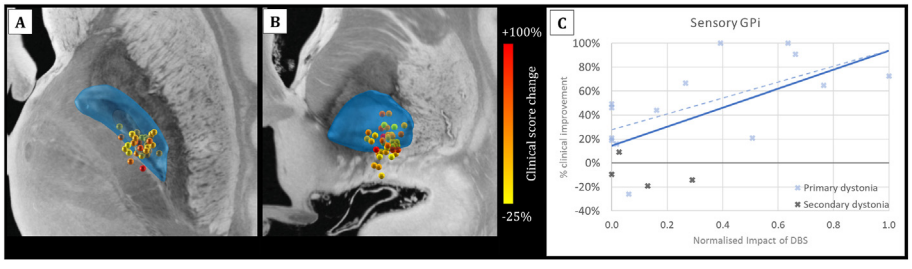

Fig. 1. DBS electrode placement and clinical correlation in eligible dystonia subjects. A, B) 3D point clouds of active stimulation contacts of individual subjects [cathode contact depicted in one subject with bipolar stimulation] overlayed over 3D reconstruction of the right internal globus pallidus (GPi) (depicted in blue) and ultra-high resolution ex vivo 7-T MRI brain scan [37]. A) viewed in the inferior-superior direction (from below), B) viewed in the anterior-posterior direction (from the front). Stimulation contacts from the left hemisphere were non-linearly flipped to the right hemisphere; right hemisphere contacts depicted as are. Colour coding (yellow-red) represents the percentual clinical score change of DBS against the pre-implantation condition. **C)** Scatterplot of percentual clinical score change (axis y) vs the min-max normalised Impact of DBS (axis x) for the sensory part of GPi with a linear trendline overlaid. The scatterplot distinguishes between primary (blue) and secondary (black) dystonia subjects and provides two trendlines – full line for all the eligible dystonia subjects and dashed line for primary dystonia patients only. Abbreviations: GPi – internal globus pallidus; DBS – deep brain stimulation. (For interpretation of the references to colour in this figure legend, the reader is referred to the Web version of this article.)

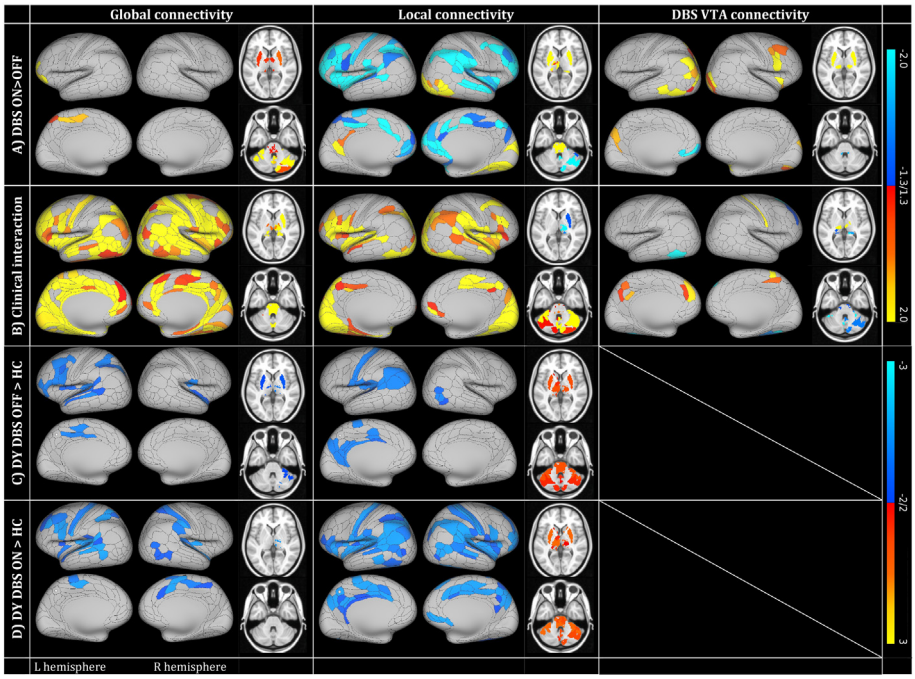

Fig. 2. Main results of resting-state functional MRI (rs-fMRI) analysis for parcellated Global Connectivity, Local Connectivity and seed-based connectivity of Volume of Tissue Activated (VTA) in deep brain stimulation (DBS) settings. **A)** Comparison of the DBS-ON session > DBS-OFF session in dystonia subjects. **B)** Interaction of the DBS-ON vs DBS-OFF contrast with the percentual clinical score change (relevant clinical scale before DBS implantation and immediately before the DBS-ON MRI session). **C)** Contrast dystonia DBS-OFF session > healthy controls. **D)** Contrast dystonia DBS-ON session > healthy controls. Alpha of 0.05 (i.e. -log(p) > 1.3) for A) and B) and 0.01 (-log(p) > 2.0), false discovery rate corrected (combined over voxels/vertices, contrasts and modalities). Subcortical structures shown in two slices z = 3 and z = −33 (MNI coordinate system). Laterality convention where the right side of the figure corresponds to the right side of the brain is used. See Table 2 and Supplementary Tables 3 and 4 for further anatomical and statistical information on significant regions. Abbreviations: DBS − deep brain stimulation; VTA − Volume of Tissue Activated; L − left; R − right.

improvement of clinical condition and DBS-ON vs. DBS-OFF contrast in right putamen and thalamus (see Fig. 3A.II) and positive interaction in multiple cortical areas (see Fig. 2B and 3.A.IV), many of them overlapping with the DBS-induced decrease of LocCon (see Aim 2 and Fig. 2B). And lastly, VTA-Con showed positive interaction of the effect of DBS and clinical score change in both thalami, cingulate cortices and right sensorimotor cortex, and negative interaction in several smaller areas in the cerebellum and both hippocampi.

4. Discussion

The presented open-label fixed-order study with cross-sectional validation against HC is, to the best of our knowledge, the first rs-fMRI investigation into the effects of DBS in dystonia. There are several conclusions of interest to be drawn from our results: firstly, the Impact of DBS for the sensory part of GPi showed a statistically significant and much stronger correlation with the clinical picture than that of the motor part of GPi. And secondly, while GPi DBS seemed to restore healthy functional connectivity, LocCon behaved in a slightly counter-intuitive way − GPi DBS induced alterations in the opposite direction when compared to the "norm" as detected in HC.

4.1. Clinical characteristics of the cohort and DBS electrode placement

There is a multitude of factors shaping the outcome of dystonia treatment, be it oral medication, botulinum toxin or GPi DBS. The aetiology of dystonia, the time elapsed since the clinical onset and severity of the clinical picture seem to affect both the clinical course and response to DBS to a substantial extent. Moreover, in DBS, the position of the electrodes in the target region plays a major role. Even if limited by relatively low subject number, our data confirmed the well-known importance of correct targeting in DBS planning. Even the dominance of sensory part of GPi over the clinical effect found in this study is not a surprise, given the hypothesised dysfunction of sensorimotor integration as the pathophysiological basis of dystonia [2]. Furthermore, the tendency to use the distal DBS electrode contacts for stimulation and exert the DBS effect in the inferior parts of the GPi or even below it is well in accord with a recently published large, multicentric meta-analysis showing the hot spot for clinical effect in this very region [27], even though not all reports agree with this localisation [28]. The disease aetiology also must not be forgotten as a major factor for GPi DBS success, even more in the context of the presented cohort − while the outcomes of DBS treatment in DYT-TOR1 patients and patients with isolated dystonia without known monogenic cause are generally favourable [29], the response in dystonias of other aetiologies is less predictable, making the selection of suitable DBS candidates challenging [30].

Indeed, "secondary" DY patients in the presented study fared worse in the clinical outcomes than their "primary" counterparts − three of the four secondary DY patients were considered non-responders by their attending physician and their clinical scores generally mildly worsened when compared to the pre-implantation condition (see Table 1). While no formal statistical comparison between the group of primary and secondary DY patients in this study is possible due to the low subject number in the latter cohort, the scatterplots in Figs. 1 and 3 show that the positioning of the electrodes and individual rs-fMRI metrics in the secondary DY group cannot be considered strong outliers and their exclusion led to only minor alterations of correlation trendline slopes (dashed lines in Fig. 1C and 3.A). Furthermore, such

Table 2
Abbreviated results of parcellated analysis of resting-state functional MRI (Global Connectivity, Local Connectivity and seed-based connectivity of the region of Volume of Tissue Activated by deep brain stimulation) for the comparison of DBS-ON vs DBS-OFF session in dystonia subjects and the interaction of the contrast DBS-ON vs. DBS-OFF with the percentual clinical score change (relevant clinical scale before DBS implantation and immediately before the DBS-ON MRI session). Data reported as parcel groups, with cortical anatomical localisation based on 22 main cortical segments and parcellation as defined by (Glasser et al., 2016) (only the first 5 most significant cortical parcels reported in groups containing more parcels), number of parcellation regions of interest contained in each parcel group, T statistic of permutation-based T test and p value in -log(p) format. Alpha of 0.05 (i.e. -log(p) > 1.3), False Discovery Rate corrected (combined over voxels/vertices, contrasts and modalities) was implemented. See Figs. 2 and 3 and Supplementary Table 3 for more information, including relevant ranges of respective metrics. Abbreviations: Mod – modality; Cntr – contrast; Lat – lateralisation; ROI – region of interest; T stat – T statistic; FDR – False Discovery Rate; L – left; R – right; C – central; DBS – deep brain stimulation; VTA – Volume of Tissue Activated.

	Mod	Cntr	Lat	Anatomical localisation	ROI no	T stat	-log(p) (FDR)
DBS ON > OFF	**Global Connectivity**	**DBS ON > DBS OFF**	R	Diencephalon ventral	1	8.101	2.500
			R	Cerebellum	4	5.584	2.500
			L	Orbital and Polar Frontal Cortex, Dorsolateral Prefrontal Cortex, Inferior Frontal Cortex	4	5.367	2.500
			L	Cerebellum	2	3.995	2.500
			C	Brainstem	2	3.701	2.178
			R	Putamen	1	3.171	1.654
			L	Paracentral Lobular and Mid Cingulate Cortex, Superior Parietal and IPS	3	3.063	1.820
			L	Thalamus	1	2.930	1.436
			R	Thalamus	1	2.859	1.403
			L	Putamen	1	2.660	1.438
	Local Connectivity	**DBS ON > DBS OFF**	C	Brainstem	5	6.436	2.500
			R	Diencephalon ventral	1	5.608	2.500
			R	MT + Complex and Neighboring Visual Areas, Ventral Stream Visual Cortex, Early Visual Cortex, Medial Temporal	14	5.372	2.500
			L	Thalamus	4	5.017	2.500
			L	Diencephalon ventral	2	4.084	2.500
			L	Putamen	1	4.012	2.089
			R	Hippocampus	1	3.725	2.089
			L	Posterior Cingulate	3	3.693	2.178
			R	Putamen	1	3.554	2.178
		DBS ON < DBS OFF	R	Anterior Cingulate, Dorsolateral Prefrontal Cortex, Inferior Parietal Cortex, Insular Cortex, Orbital and Polar Frontal Cortex …	45	−8.323	2.500
			L	Insular Cortex, Superior Parietal and IPS, Inferior Frontal Cortex, Orbital and Polar Frontal Cortex, Dorsolateral Prefrontal Cortex, Inferior Parietal Cortex …	48	−6.332	2.500
			R	Posterior Cingulate, Paracentral Lobular and Mid Cingulate Cortex, Superior Parietal and IPS	6	−4.548	2.500
			R	Auditory Association Cortex	4	−4.523	2.500
			L	Anterior Cingulate	3	−4.443	2.500
			L	Anterior Cingulate, Dorsolateral Prefrontal Cortex, Orbital and Polar Frontal Cortex	5	−4.355	2.500
			R	Cerebellum	2	−4.004	2.500
	DBS VTA connectivity	**DBS ON > DBS OFF**	L	Thalamus	1	7.176	2.500
			R	Insular Cortex	3	6.382	2.500
			R	Thalamus	1	5.796	2.500
			R	Early Visual Cortex, MT + Complex and Neighboring Visual Areas	4	5.038	2.500
			L	MT + Complex and Neighboring Visual Areas, Inferior Parietal Cortex, Lateral Temporal Cortex, Temporal-Parietal-Occipital Junction	8	4.980	2.500
			R	Cerebellum	1	4.643	2.500
			R	Putamen	1	4.410	2.500
			R	Premotor Cortex, Dorsolateral Prefrontal Cortex, Inferior Frontal Cortex	4	4.258	2.500
			L	Posterior Cingulate, Superior Parietal and IPS, Dorsal Stream Visual Cortex	5	3.868	2.303
			L	Putamen	1	3.842	2.303
		DBS ON < DBS OFF	L	Anterior Cingulate, Orbital and Polar Frontal Cortex	3	−4.039	2.500
			C	Brainstem	1	−2.984	1.753
			L	Diencephalon ventral	1	−2.706	1.395
Interaction ON > OFF vs clinical improvement	Global Connectivity	positive	R	Insular Cortex, Posterior Cingulate, Anterior Cingulate, Dorsolateral Prefrontal Cortex, Inferior Parietal Cortex, Premotor Cortex, …	121	11.673	2.500
			C	Brainstem	8	11.630	2.500
			L	Anterior Cingulate, Posterior Cingulate, Insular Cortex, Superior Parietal and IPS, Inferior Frontal Cortex …	114	10.269	2.500
			R	Amygdala	3	9.497	2.500
			R	Putamen	1	8.926	2.500
			L	Hippocampus	2	7.189	2.500
			R	Diencephalon ventral	3	6.619	2.500
			R	Hippocampus	4	6.424	2.500
			R	Thalamus	4	6.278	2.500
			L	Putamen	1	4.676	2.500
			L	Amygdala	2	4.300	2.500
			R	Cerebellum	1	3.984	2.303
			L	Cerebellum	2	3.609	2.178
			L	Thalamus	2	3.409	2.025
			L	Diencephalon ventral	1	3.389	1.787
	Local Connectivity	**positive**	L	Ventral Stream Visual Cortex, Dorsal Stream Visual Cortex, Medial Temporal, Posterior Cingulate, MT + Complex and Neighboring Visual Areas …	37	11.219	2.500
			R	Insular Cortex, Inferior Parietal Cortex, Dorsal Stream Visual Cortex, Ventral Stream Visual Cortex ….	58	7.185	2.500
			L		30	6.116	2.500

Table 2 (*continued*)

Mod	Cntr	Lat	Anatomical localisation	ROI no	T stat	-log(p) (FDR)
			Insular Cortex, Inferior Frontal Cortex, Auditory Association Cortex, Early Auditory Cortex, Orbital and Polar Frontal Cortex …			
		R	Cerebellum	6	5.017	2.500
		L	Cerebellum	6	5.008	2.500
		R	Dorsolateral Prefrontal Cortex, Premotor Cortex	3	4.883	2.500
		R	Posterior Cingulate, Paracentral Lobular and Mid Cingulate Cortex, Anterior Cingulate	6	3.948	2.500
		C	Brainstem	2	3.163	1.674
		R	Anterior Cingulate	3	3.052	1.964
	negative	R	Amygdala	1	−4.419	2.500
		R	Thalamus	3	−3.892	2.500
		R	Putamen	1	−2.590	1.395
DBS VTA connectivity	**positive**	R	Thalamus	1	10.341	2.500
		R	Paracentral Lobular and Mid Cingulate Cortex, Somatosensory and Motor Cortex	3	5.486	2.500
		L	Putamen	1	5.388	2.500
		L	Thalamus	1	5.011	2.500
		L	Anterior Cingulate, Dorsolateral Prefrontal Cortex	3	3.294	1.906
		L	Posterior Cingulate	3	3.082	1.787
	negative	L	Diencephalon ventral	1	−7.048	2.500
		L	Ventral Stream Visual Cortex, MT + Complex and Neighboring Visual Areas	3	−6.475	2.500
		L	Cerebellum	2	−4.467	2.500
		R	Dorsolateral Prefrontal Cortex	3	−4.462	2.500
		R	Hippocampus	3	−4.082	2.178
		R	Cerebellum	2	−3.413	2.025
		R	Ventral Stream Visual Cortex, Medial Temporal	3	−3.287	1.964
		C	Brainstem	1	−2.621	1.385
		L	Hippocampus	1	−2.562	1.427
		R	Diencephalon ventral	1	−2.558	1.347
		L	Thalamus	1	−2.459	1.406

comparison would falsely presume certain level of homogeneity in the secondary DY group, which included two Parkinson-plus syndrome cases, one PKAN and one post-anoxic DY patient. But by the same token, the putative homogeneity in the idiopathic primary DY patients may also be questioned, given the unknown true aetiology of the disease in this subgroup. Ultimately, this “inconvenient” aetiological uncertainty provides a viable backing for the heterogeneity of the studied DY group - while the underlying neuropathological cascade leading to dystonic symptoms differs among the study participants, introducing an unwanted bias and posing a possible limitation to the presented study, the similarity of the clinical dystonic phenotype could be considered an indication of a viably common substrate at the level of central nervous system processing pathways and of a common principle of GPi DBS mechanisms of action. Nonetheless, the need for the use of two clinical scales (TWSTRS and BFMDS) to evaluate DBS-related clinical improvement of phenotypically different dystonia presentations, even though utilised as a percentual clinical improvement of relevant scale in comparison with the pre-implantation state, is a limitation difficult to account for and calls for certain caution in the interpretation of the results of the presented study. Ultimately, similar studies focusing on more coherent clinical entities may shed further light on this issue.

4.2. rs-fMRI metrics – ambiguous restoration of healthy network state

In accordance with our hypothesis, active GPi DBS partly restored healthy network connectivity (GloCon) mainly in the subcortical structures as putamen, thalamus, ventral diencephalon and cerebellum, with seemingly minimal effects on cortical regions (see Fig. 2B and 3.B and Table 2). However, the interaction of DY DBS-ON vs DY DBS-OFF contrast against the clinical score change revealed a strong positive relationship with the clinical improvement spread over large-scale cortical regions bilaterally and to a lesser extent also in the subcortical structures (see Fig. 2B and 3.A.I and 3.A.III and Table 2). This notion of DBS being able to re-establish network states present in healthy brains is generally in accord with the hypothesised mechanism of action of subthalamic nucleus DBS reported in Parkinson's disease [16]. Nonetheless, GPi DBS induced an increase of LocCon in basal ganglia and brainstem and cortical LocCon decrease to states farther from the condition detected in HC. Moreover, the farther LocCon strayed from the “norm” as found in HC, the worse was the clinical effect of DBS in individual subjects (see Fig. 3A.II and 3.A.IV). However, this also means that the better the DY subjects responded to GPi DBS clinically, the smaller this effect was and the best responders, represented by data points at the top of y-axis in Fig. 3.AII and 3.A.IV, resisted this group-level finding and tended to restore their respective LocCon values towards the HC level. This apparent discordance with the group-level findings (DBS-ON vs DBS-OFF contrast) might even be associated with the general diversity of clinical outcomes in GPi DBS in dystonia. In this context, one must consider the utilisation of the clinical scale change based on the difference of the score before DBS implantation and before the DBS-ON session, leaving a rather long period for further disease progression – dystonia associated with neurodegeneration (PKAN and Parkinson-plus patients - three in total) might have been affected by ongoing pathological processes in the brain. However, the use of the clinical score change associated with acute deactivation of GPi DBS (the score before DBS-ON session and the score before DBS-OFF session, with the interval of 2 h) would be oblivious to the slow, long-term changes induced by GPi DBS in dystonia [9,10], where weeks are often necessary to see an effect of DBS parameter adjustments. This very nature of DBS programming in clinical settings also makes the design of research studies into GPi DBS effects problematic – the modification of DBS parameters is essentially heuristic, based on clinical records and often on trial-by-trial basis. Given the general aim of the study, forceful unification of stimulation parameters would disregard the individual differences in clinical needs of patients, DBS lead position and possibly also the sensitivity of each patient to DBS settings.

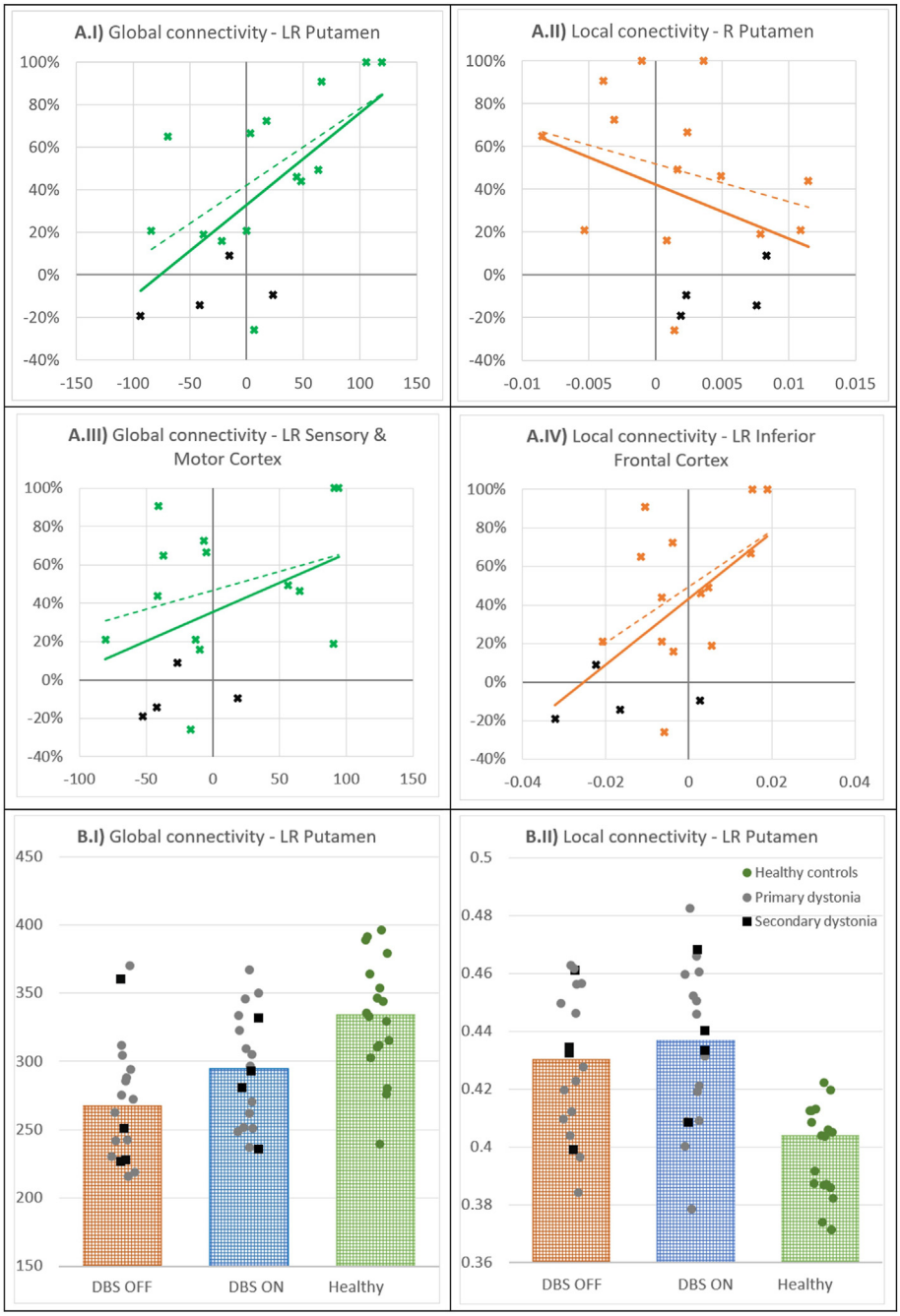

Fig. 3. Correlation of MRI metrics with clinical score change and comparison to healthy controls. A) Scatterplots of percentual clinical score change (axis y) vs the DBS-induced change of resting-state functional MRI parameters (axis x) calculated as the value of the parameter of interest in the DBS-ON session minus its value in DBS-OFF session for the respective area. Both Local Connectivity (LocCon) (orange) and Global Connectivity (GloCon) (green) presented for the putamen (A.I and A.II). A.III depicts the correlation of GloCon difference with clinical score change in bilateral sensory and motor cortex; A.IV the LocCon correlation in bilateral inferior frontal cortex. The scatterplots distinguish between primary (green for GloCon and orange for LocCon) and secondary (black) dystonia subjects. Linear trendlines are overlaid in scatterplots – full line for all the eligible dystonia subjects and dashed line for primary dystonia patients only. **B)** Comparison of GloCon and LocCon in putamen in dystonia DBS-OFF and DBS-ON session and in healthy controls. Columns represent medians of respective sessions/groups, points with mild jitter of the main column axis for better visibility correspond to individual subjects. Black squares mark secondary dystonia subjects. Abbreviations: DBS – deep brain stimulation; R – right; LR – left and right. (For interpretation of the references to colour in this figure legend, the reader is referred to the Web version of this article.)

The localisation of detected DBS-induced network alterations provides important clues on its mechanism of action as well. While definitely limited by MRI artifacts associated with the presence of the DBS system itself and utilised masking unfortunately removing areas of much interest such as both pallida and large parts of left-side sensorimotor cortex (see Supplementary Figure 2B,C), the repeated emergence of putamina, thalami, brainstem and cerebellar structures points to their crucial position in both the effect of DBS (see Fig. 2B), but also in the pathophysiology of dystonia (see Fig. 3A). This is in line with previous literature showing abnormal metabolism in basal ganglia, thalamus, cerebellum and also sensorimotor cortex in focal dystonia, differences of volume, but also in various rs-fMRI metrics in these areas [6,31,32]. Interestingly, also the alterations in visual cortex emerging in the

interaction analysis of DBS effect vs. clinical improvement in this study are not a new notion – differences in visual, but also executive control networks in cervical dystonia [33] and in default-mode network in blepharospasm [34] are well in accord with our findings. And lastly, higher VTA-con in DBS-ON condition in both putamina and thalami casts some further light on the inner underpinnings of GPi signal modifications induced by DBS, but must definitely be taken with a grain of salt due to poor signal quality in the VTA region in close vicinity of the electrodes, though the bilaterality of the subcortical finding allows for some confidence.

In addition to the above and the already described limitations associated with the clinical heterogeneity of the study population, further word of caution is necessary towards the inherently altered fMRI data quality due to the presence of artifacts. Despite the numerous mitigation measures described in the Supplementary material, the inter-individual differences in metal-related off-resonance artifact size and positions may introduce bias not only in the comparison between dystonia subjects and HC, but also DBS ON and DBS OFF state. Advanced zero echo time sequences will definitely be of interest in this area in the future [35]. Furthermore, the relatively short delay between the DBS ON and DBS OFF fMRI acquisitions in this study does not allow for full elimination of long-term GPi DBS effects related to neural plasticity [36], calling for further caution in the interpretation of the presented study. A well-designed, longitudinal protocol would be apt to provide more complete information on this matter. And lastly, DBS-related structural alterations may be of substantial interest in further studies. Unfortunately, non-negligible preimplantation MRI protocol differences in the presented cohort (see Supplementary Table 1) did not allow for the analysis of this important aspect.

5. Conclusion

GPi DBS leads to the restoration of GloCon patterns towards those of HC, with positive direct correlation in the cortico-basal ganglia-thalamo-cortical and cerebellar networks with the clinical improvement. Nonetheless, on average, GPi DBS also seemed to bring LocCon both in the cortical and subcortical regions farther away from the state detected in HC. However, LocCon in better DBS responders defied this effect, as seen in based on its correlation with clinical outcome, approached the connectivity seen HC. All in all, the extent of restoration of both these main metrics of interest towards the normal HC levels clearly correlates with the clinical improvement showing that the restoration of physiological network state may be a precondition for successful DBS outcome in dystonia.

Funding statement

Support was provided by the Czech Ministry of Health (AZV NV19-04-00233), under the frame of EJP RD, the European Joint Programme on Rare Diseases (EJP RD COFUND-EJP N° 825575), by the National Institute for Neurological Research, Czech Republic, Programme EXCELES, ID Project No. LX22NPO5107, funded by the European Union – Next Generation EU and also by the Charles University: Cooperatio Program in Neuroscience.

Data availability

The MRI datasets of the presented study are not publicly available due to the sensitive nature and data privacy regulations related to patient data. However, they are available from the corresponding author upon reasonable request.

Code availability

Not applicable.

Authors' contributions

P.F. designed the data analysis approach, performed the data analysis, created the figures and tables and wrote the manuscript. R.J. designed the study protocol, managed the patient enrolment, monitored the data acquisition and edited the manuscript. A.F. managed the patient enrolment, monitored the data acquisition and edited the manuscript. P.H. and F.R. managed the patient enrolment and revised the manuscript. K.M. designed the study protocol and revised the manuscript. D.U. designed the study protocol and revised the manuscript.

Ethics approval

The study protocol was approved by the ethics committee of the General University Hospital in Prague, Czech Republic.

Consent to participate

Each subject provided a written informed consent in accordance with the Declaration of Helsinki.

Declaration of competing interest

The authors declare that they have no known competing financial interests or personal relationships that could have appeared to influence the work reported in this paper.

Acknowledgements

The authors wish to express their sincere thanks to the patients and their families for their support of research activities.

Financial support for this project was provided by the General University Hospital in Prague (MH CZ-DRO-VFN64165), Czech Ministry of Health (AZV NV19-04-00233) under the frame of EJP RD, the European Joint Programme on Rare Diseases (EJP RD COFUND-EJP N° 825575), by the National Institute for Neurological Research, Czech Republic, Programme EXCELES, ID Project No. LX22NPO5107, funded by the European Union – Next Generation EU and also by the Charles University: Cooperatio Program in Neuroscience.

Appendix A. Supplementary data

Supplementary data to this article can be found online at https://doi.org/10.1016/j.brs.2022.08.025.

References

[1] Albanese A, Bhatia K, Bressman SB, DeLong MR, Fahn S, Fung VSC, et al. Phenomenology and classification of dystonia: a consensus update. Mov Disord 2013;28(7):863–73.
[2] Balint B, Mencacci NE, Valente EM, Pisani A, Rothwell J, Jankovic J, et al. Dystonia. Nat Rev Dis Primers 2018;4(1):1–23.
[3] Egger K, Mueller J, Schocke M, Brenneis C, Rinnerthaler M, Seppi K, et al. Voxel based morphometry reveals specific gray matter changes in primary dystonia. Mov Disord 2007;22(11):1538–42.
[4] Pantano P, Totaro P, Fabbrini G, Raz E, Contessa GM, Tona F, et al. A transverse and longitudinal MR imaging voxel-based morphometry study in patients with primary cervical dystonia. Am J Neuroradiol 2011;32(1):81–4.
[5] Gonzalez-Escamilla G, Muthuraman M, Reich MM, Koirala N, Riedel C, Glaser M, et al. Cortical network fingerprints predict deep brain stimulation outcome in dystonia. Mov Disord 2019;34(10):1537–46.

[6] Simonyan K. Neuroimaging applications in dystonia. Int Rev Neurobiol 2018;143:1–30.
[7] Chiken S, Nambu A. Mechanism of deep brain stimulation: inhibition, excitation, or disruption? Neuroscientist 2016;22(3):313–22.
[8] Kupsch A, Benecke R, Müller J, Trottenberg T, Schneider GH, Poewe W, et al. Pallidal deep-brain stimulation in primary generalized or segmental dystonia. N Engl J Med 2006;355(19):1978–90.
[9] Ruge D, Tisch S, Hariz MI, Zrinzo L, Bhatia KP, Quinn NP, et al. Deep brain stimulation effects in dystonia: time course of electrophysiological changes in early treatment. Mov Disord 2011;26(10):1913–21.
[10] Ruge D, Cif L, Limousin P, Gonzalez V, Vasques X, Hariz MI, et al. Shaping reversibility? Long-term deep brain stimulation in dystonia: the relationship between effects on electrophysiology and clinical symptoms. Brain 2011;134(7):2106–15.
[11] Herrington TM, Cheng JJ, Eskandar EN. Mechanisms of deep brain stimulation. J Neurophysiol 2016;115(1):19–38.
[12] Burke RE, Fahn S, Marsden CD, Bressman SB, Moskowitz C, Friedman J. Validity and reliability of a rating scale for the primary torsion dystonias. Neurology 1985;35(1):73. 73.
[13] Consky ES, Basinski A, Belle L, Ranawaya R, Lang AE. The Toronto Western spasmodic Torticollis rating scale (TWSTRS): assessment of validity and inter-rater reliability. Neurology 1990;40(Suppl 1):445.
[14] Horn A, Kühn AA. Lead-DBS: a toolbox for deep brain stimulation electrode localizations and visualizations. Neuroimage 2015;107:127–35.
[15] Horn A, Li N, Dembek TA, Kappel A, Boulay C, Ewert S, et al. Lead-DBS v2: towards a comprehensive pipeline for deep brain stimulation imaging. Neuroimage 2019;184:293–316.
[16] Horn A, Wenzel G, Irmen F, Huebl J, Li N, Neumann WJ, et al. Deep brain stimulation induced normalization of the human functional connectome in Parkinson's disease. Brain 2019;142(10):3129–43.
[17] Glasser MF, Sotiropoulos SN, Wilson JA, Coalson TS, Fischl B, Andersson JL, et al. The minimal preprocessing pipelines for the Human Connectome Project. Neuroimage 2013;80:105–24.
[18] Smith SM, Beckmann CF, Andersson J, Auerbach EJ, Bijsterbosch J, Douaud G, et al. Resting-state fMRI in the human connectome project. Neuroimage 2013;80:144–68.
[19] Salimi-Khorshidi G, Douaud G, Beckmann CF, Glasser MF, Griffanti L, Smith SM. Automatic denoising of functional MRI data: combining independent component analysis and hierarchical fusion of classifiers. Neuroimage 2014;90:449–68.
[20] Cox RW. AFNI: software for analysis and visualization of functional magnetic resonance neuroimages. Comput Biomed Res 1996;29(3):162–73.
[21] Craddock RC, Clark DJ. Optimized implementations of voxel-wise degree centrality and local functional connectivity density mapping in AFNI. Gigascience [Internet]. 2016 Nov 1 [cited 2020 Jul 11];5(suppl_1). Available from: https://academic.oup.com/gigascience/article/5/suppl_1/s13742-016-0147-0-d/2965209.
[22] Zang Y, Jiang T, Lu Y, He Y, Tian L. Regional homogeneity approach to fMRI data analysis. Neuroimage 2004 May;22(1):394–400.
[23] Glasser MF, Coalson TS, Robinson EC, Hacker CD, Harwell J, Yacoub E, et al. A multi-modal parcellation of human cerebral cortex. Nature 2016;536(7615):171–8.
[24] Benjamini Y, Hochberg Y. Controlling the false discovery rate: a practical and powerful approach to multiple testing. J Roy Stat Soc B 1995;57(1):289–300.
[25] Winkler AM, Webster MA, Brooks JC, Tracey I, Smith SM, Nichols TE. Non-parametric combination and related permutation tests for neuroimaging. Hum Brain Mapp 2016;37(4):1486–511.
[26] Ewert S, Plettig P, Li N, Chakravarty MM, Collins DL, Herrington TM, et al. Toward defining deep brain stimulation targets in MNI space: a subcortical atlas based on multimodal MRI, histology and structural connectivity. Neuroimage 2018;170:271–82.
[27] Reich MM, Horn A, Lange F, Roothans J, Paschen S, Runge J, et al. Probabilistic mapping of the antidystonic effect of pallidal neurostimulation: a multicentre imaging study. Brain 2019;142(5):1386–98.
[28] Okromelidze L, Tsuboi T, Eisinger RS, Burns MR, Charbel M, Rana M, et al. Functional and structural connectivity patterns associated with clinical outcomes in deep brain stimulation of the globus pallidus internus for generalized dystonia. Am J Neuroradiol 2020;41(3):508–14.
[29] Brüggemann N, Kühn A, Schneider SA, Kamm C, Wolters A, Krause P, et al. Short- and long-term outcome of chronic pallidal neurostimulation in monogenic isolated dystonia. Neurology 2015 Mar 3;84(9):895–903.
[30] Andrews C, Aviles-Olmos I, Hariz M, Foltynie T. Which patients with dystonia benefit from deep brain stimulation? A metaregression of individual patient outcomes. J Neurol Neurosurg Psychiatr 2010 Dec 1;81(12):1383–9.
[31] Poston KL, Eidelberg D. Functional brain networks and abnormal connectivity in the movement disorders. Neuroimage 2012 Oct 1;62(4):2261–70.
[32] Fečíková A, Jech R, Čejka V, Čapek V, Šťastná D, Štětkářová I, et al. Benefits of pallidal stimulation in dystonia are linked to cerebellar volume and cortical inhibition. Sci Rep 2018;8(1):1–14.
[33] Delnooz CC, Pasman JW, Beckmann CF, van de Warrenburg BP. Task-free functional MRI in cervical dystonia reveals multi-network changes that partially normalize with botulinum toxin. PLoS One 2013;8(5):e62877.
[34] Yang J, Luo C, Song W, Chen Q, Chen K, Chen X, et al. Altered regional spontaneous neuronal activity in blepharospasm: a resting state fMRI study. J Neurol 2013;260(11):2754–60.
[35] Lehto LJ, Filip P, Laakso H, Sierra A, Slopsema JP, Johnson MD, et al. Tuning neuromodulation effects by orientation selective deep brain stimulation in the rat medial frontal cortex. Front Neurosci [Internet]. 2018 [cited 2021 Jul 31];0. Available from: https://www.frontiersin.org/articles/10.3389/fnins.2018.00899/full.
[36] Hemm S, Vayssiere N, Mennessier G, Cif L, Zanca M, Ravel P, et al. Evolution of brain impedance in dystonic patients treated by GPi electrical stimulation. Neuromodulation: Technol Neural Interf 2004 Apr 1;7(2):67–75.
[37] Edlow BL, Mareyam A, Horn A, Polimeni JR, Witzel T, Tisdall MD, et al. 7 Tesla MRI of the ex vivo human brain at 100 micron resolution. Sci Data 2019;6(1):1–10.